

RESEARCH ARTICLE

Front-signal-dependent accumulation of the RHOA inhibitor FAM65B at leading edges polarizes neutrophils

Kun Gao^{1,2,*}, Wenwen Tang^{2,*}, Yuan Li², Pingzhao Zhang^{1,3}, Dejie Wang¹, Long Yu^{1,3}, Chenji Wang^{1,‡} and Dianqing Wu^{2,‡}

ABSTRACT

A hallmark of neutrophil polarization is the back localization of active RHOA and phosphorylated myosin light chain (pMLC, also known as MYL2). However, the mechanism for the polarization is not entirely clear. Here, we show that FAM65B, a newly identified RHOA inhibitor, is important for the polarization. When FAM65B is phosphorylated, it binds to 14-3-3 family proteins and becomes more stable. In neutrophils, chemoattractants stimulate FAM65B phosphorylation largely depending on the signals from the front of the cells that include those mediated by phospholipase C β (PLC β) and phosphoinositide 3-kinase γ (PI3K γ), leading to FAM65B accumulation at the leading edge. Concordantly, FAM65B deficiency in neutrophils resulted in an increase in RHOA activity and localization of pMLC to the front of cells, as well as defects in chemotaxis directionality and adhesion to endothelial cells under flow. These data together elucidate a mechanism for RHOA and pMLC polarization in stimulated neutrophils through direct inhibition of RHOA by FAM65B at the leading edge.

KEY WORDS: Chemotaxis, RHOA, Polarization, FAM65B, Neutrophil

INTRODUCTION

Cell polarization is a fundamental, but not yet fully understood, biological process that is crucially important for many cellular functions, including cell migration (Iden and Collard, 2008; Onsum and Rao, 2009). Circulating naive neutrophils are apolar, but upon stimulation by chemoattractants they rapidly polarize in a manner that is epitomized by formation of lamellar-type F actin at the front and localization of active RHOA and phosphorylated myosin light chain (pMLC, also known as MYL2) at the back (Bourne and Weiner, 2002; Graziano and Weiner, 2014; Liu and Parent, 2011; Wang, 2009; Wu, 2005). It remains, however, incompletely understood how RHOA activation and pMLC localization is polarized. Rho guanine-nucleotide-exchange factors (GEFs) are the immediate upstream activators of

RHOA, and one of them, PDZRhoGEF (also known as ARHGEF11) is localized at the back of differentiated HL-60 neutrophil-like cells to activate RHOA there (Wong et al., 2007). Paradoxically, Lfc (also known as ARHGEF2 and GEF115), a RHOA GEF that is largely responsible for chemoattractant-stimulated RHOA activation in mouse neutrophils, based on genetic study, shows no polarized localization and is localized at both the front and back of stimulated mouse neutrophils (Francis et al., 2006). Another explanation for RHOA polarization in neutrophils is the mutual antagonism between RHOA and RAC (Srinivasan et al., 2003), a phenomenon observed in many different types of cells (Iden and Collard, 2008). The molecular mechanisms for this antagonism seem to be dependent on the cell context (Iden and Collard, 2008), and that underlying the antagonism in mouse neutrophils is not clear. In addition, studies in HL-60 differentiated neutrophil-like cells and zebrafish neutrophils have revealed RAC-independent, but phosphoinositide 3-kinase (PI3K)-dependent, mechanisms for the regulation of RHOA and pMLC (Van Keymeulen et al., 2006; Yoo et al., 2010). Moreover, a mammalian target of rapamycin complex 2 (mTORC2) to adenylate cyclase 9 (AC9, also known as ADCY9) pathway has been shown to exclude cAMP from the front and regulate RHOA and pMLC, probably in a protein kinase C (PKC)-dependent mechanism (Liu et al., 2010). Disruption of this pathway results in increased pMLC at the front of the cell. However, all of these aforementioned mechanisms have significant missing links: how PI3K regulates RHOA and pMLC; how mTORC2 and PKC excludes cAMP from the front; and how PDZRhoGEF polarizes to the back. The back localization of PDZRhoGEF, whose significance in mouse neutrophil polarization remains undetermined, is presumably the result of cell polarization and might also depend on the front signals.

FAM65B (also known as C6ORF32, KIAA0386, and PL48), whose mRNA level is known to be upregulated during DMSO-induced HL-60 cell differentiation (Dakour et al., 1997), induces the formation of neurite-like protrusions when overexpressed in HEK293 and C2C12 cells (Hirayama and Kim, 2008; Yoon et al., 2007). It belongs to the FAM65 family of proteins, which is also included FAM65A and FAM65C. Recently, FAM65B has been shown to be a RHOA inhibitor (Rougerie et al., 2013). It directly binds to RHOA and blocks the loading of GTP to RHOA. It was also shown that it has a role in chemokine-stimulated migration and adhesion of Jurkat cells (Rougerie et al., 2013). In this study, we confirm FAM65B as being a RHOA inhibitor. In addition, we found that FAM65B, when phosphorylated, binds to 14-3-3 proteins, resulting in its stabilization. Moreover, we demonstrate that FAM65B mediates a front-signal-dependent polarization of active RHOA and pMLC in neutrophils.

¹State Key Laboratory of Genetic Engineering, Collaborative Innovation Center for Genetics and Development, Institute of Genetics, School of Life Sciences, Fudan University, 220 Handan Road, Shanghai 200433, P.R. China. ²Vascular Biology and Therapeutic Program, Department of Pharmacology, Yale University School of Medicine, 10 Amistad Street, New Haven, CT 06410, USA. ³Institutes of Biomedical Sciences, Fudan University, Shanghai, 200032, P. R. China. *These authors contributed equally to this work

[‡]Authors for correspondence (chenjiwang@fudan.edu.cn; dan.wu@yale.edu)

Received 8 August 2014; Accepted 6 January 2015

RESULTS

To characterize proteins that might interact with FAM65B, a HEK293 cell line was established to stably express FAM65B carrying both FLAG and HA tags. After tandem affinity purification using anti-FLAG and anti-HA antibodies, the eluent was subjected to SDS-PAGE separation followed by protein staining. Three of the most prominent bands (Fig. 1A) were excised for mass spectrometry (MS) analysis. FAM65B, 14-3-3

proteins (including isoforms of α , β , γ , θ , δ , η , ϵ , and ζ), and RHOA were identified with the high confidence from each of the bands, respectively, as indicated in Fig. 1A. We performed co-immunoprecipitation to verify the interactions of FAM65B with RHOA and 14-3-3 proteins. FAM65B co-immunoprecipitated with endogenous RHOA, but not CDC42 or RAC1, in HEK293 cells (Fig. 1B). We also detected co-immunoprecipitation of FAM65B with endogenous 14-3-3 proteins (Fig. 1B).

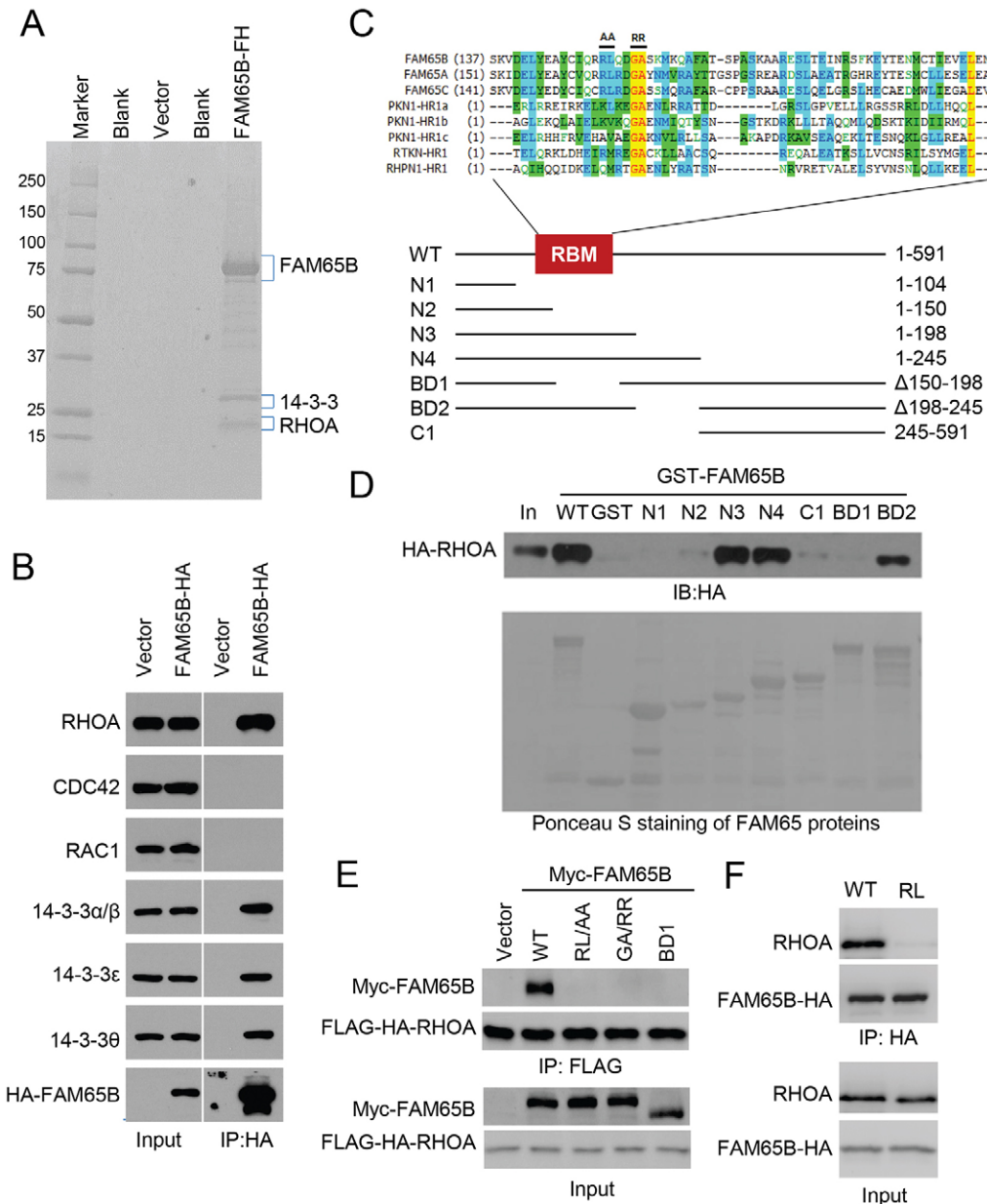


Fig. 1. Identification of proteins that bind to FAM65B. (A) SDS-PAGE separation of proteins eluted from tandem affinity purification of FAM65B. Three visible bands revealed by Coomassie Blue staining were excised for MS analysis. The highest confidence identifications are shown. (B) Co-immunoprecipitation (IP) of FAM65B with small GTPases and 14-3-3 proteins. FAM65B was precipitated using anti-HA antibody from HEK293 cells stably expressing HA-FLAG-FAM65B, and its associated proteins were detected using antibodies for small GTPase or 14-3-3 proteins as indicated. (C) Amino acid sequence alignment of the RHO-binding motif (RBM) of FAM65 proteins with the RHOA-binding homology regions (HR) of PKN1, rhotekin (RTKN) and rhophilin (RHPN1). The lower panel shows a schematic representation of FAM65B deletional mutants. (D) Interaction of recombinant GST-FAM65B with HA-RHOA expressed in HEK293 cells. IB, immunoblot. In, input. (E) Interaction of RHOA with FAM65 mutants assayed by co-immunoprecipitation in HEK293 cells. (F) Interaction of RHOA with FAM65 assayed by co-immunoprecipitation in primary mouse neutrophils transfected with FAM65B-HA. RL/AA, Arg151 and Leu152 to Ala; G/RR, Gly155 and Ala156 to Arg; RL, Arg151 and Leu152 to Ala.

Recently, Rougerie et al. have shown that FAM65B directly binds to and inhibits RHOA (Rougerie et al., 2013). We confirmed that FAM65B was a potent inhibitor of RHOA, because FAM65B overexpression reduced the amount of active RHOA detected by the RBD pulldown assay (supplementary material Fig. S1A) and inhibited RHOA-induced activation of the SRE.L reporter gene (supplementary material Fig. S1B). This SRE.L reporter gene system has previously been used to detect RHOA-mediated transcriptional activation (Hill et al., 1995; Wang et al., 2009). We also observed that recombinant FAM65B protein inhibited GTP loading to recombinant RHOA (supplementary material Fig. S1C). However, we found that the region of FAM65B (residues 54–113) previously identified as being the RHOA-binding site by Rougerie et al. (Rougerie et al., 2013) might not be the major RHOA-binding site, because the N2 fragment, which encompasses these residues, did not show a strong interaction with RHOA in comparison to wild-type (WT) or the N3 fragment (Fig. 1C,D). We instead identified a RHOA-binding motif (RBM) within the N3 fragment, but downstream of residue 113. This RBM is conserved in the FAM65 family of proteins and shares weak similarity with RHOA-binding domains in several known RHOA target proteins, including protein kinase N (PKN), rhotekin (RTKN), and rhophilin (RHPN) (Fig. 1C). FAM65B mutants lacking this motif failed to interact with RHOA (Fig. 1D). Importantly, mutation of residues Arg151 and Leu152 to Ala (conserved among three FAM65 isoforms) or Gly155 and Ala156 to Arg (conserved among all of these RHOA-binding proteins) within this motif abolished the interaction with RHOA (Fig. 1E). We also assessed the interaction of FAM65B with RHOA in mouse neutrophils. We found that heterologously expressed FAM65B and endogenous RHOA proteins co-immunoprecipitated (Fig. 1F).

A query for FAM65B in the human gene expression database BioGPS (www.biogps.org) revealed that it was highly expressed in hematopoietic cells, including neutrophils. In addition, the query also indicates that the mRNA level of FAM65B might be much higher than those of the other two FAM65 members in neutrophils. Our gene expression microarray analysis of mouse bone marrow neutrophils confirmed the finding (data not shown). Because RHOA has important roles in neutrophil polarization, chemotaxis and adhesion, we decided to investigate the importance of FAM65B in neutrophils. We obtained a FAM65B-deficient mouse line in which exons 2–14 are deleted from the Mouse Knockout Project Repository. The FAM65B-deficient mice show no gross phenotypes. Western blotting analysis of neutrophils isolated from the mutant mice showed a lack of the FAM65B protein (Fig. 2A). We used the Rho activation assay (G-LISA) to assess the effect of FAM65B-deficiency on RHOA activity in neutrophils and found that chemoattractants formyl-Met-Leu-Phe (fMLP) and chemokine (C-X-C motif) ligand 2 (CXCL2) induced significantly greater RHOA activation in FAM65B-deficient neutrophils than in WT cells at low concentrations of ligands (Fig. 2B,C; supplementary material Fig. S1D). These results are consistent with the aforementioned conclusion that FAM65B is a RHOA inhibitor. When pMLC, a surrogate marker for RHOA activity that is normally localized at the backs of stimulated neutrophils (Li et al., 2005; Li et al., 2003; Xu et al., 2003; Xu et al., 2010), was visualized using immunostaining, we found that pMLC was localized at both the front and back of a majority of FAM65B-deficient neutrophils (Fig. 2D,E). In agreement with mis-localization of pMLC and elevated RHOA activity, FAM65B-deficient

neutrophils showed defective directionality in their chemotaxis in an fMLP gradient as the mutant cells showed greater errors in following the direction of the chemoattractant gradient than the WT cells did (supplementary material Movie 1; Fig. 2F). FAM65B deficiency, by contrast, did not appear to significantly affect the motility of neutrophil migration (Fig. 2F). Moreover, FAM65B-deficiency reduced the *in vivo* recruitment of neutrophils into inflamed peritonea (Fig. 2G). Consistent with previous knowledge on the positive role of RHOA in leukocyte adhesion to endothelium (Francis et al., 2006; Giagulli et al., 2004; Honing et al., 2004; Xu et al., 2010), we observed that enhanced adhesion of FAM65B-deficient neutrophils to endothelial cells under flow (Fig. 2H).

To gain a better understanding how the loss of FAM65B results in pMLC localization at the front of polarized neutrophils, we examined the localization of FAM65B-GFP in neutrophils. To minimize cell-shape-mediated fluctuation in GFP fluorescence, we coexpressed tdTomato with FAM65B-GFP and performed ratio imaging. FAM65B was rapidly accumulated to the front of the chemotaxing neutrophils upon stimulation (Fig. 3A; supplementary material Fig. S2A). We also examined FAM65B-GFP localization in neutrophils coexpressing LifeAct-RFP, which detects polymerized actin (Riedl et al., 2008), and observed the same front localization of FAM65B-GFP (supplementary material Movie 2). Given that FAM65B inhibits RHOA activity, the front localization of FAM65B provides an explanation for the front localization of pMLC in FAM65B-deficient neutrophils, probably resulting from increased RHOA activity at the front of these mutant cells.

When we performed western blotting detection of the FAM65B protein in neutrophils, we noticed an upshift of the FAM65B bands accompanied by increases in their intensity after increasing times of chemoattractant stimulation (Fig. 3B). The aforementioned MS analysis also identified FAM65B residues 21, 37, 341, 523 and 535 as phosphorylated Ser (supplementary material Fig. S2B). These Ser residues fit the consensus binding motifs for 14-3-3 proteins, which binds to FAM65B (Fig. 1A,B). In addition, they match the substrate motifs for many protein kinases including PKC and AKT. In fact, treatment with phorbol myristate acetate (PMA), which can activate PKC, or the phosphatase inhibitor okadaic acid resulted in upshifts of the FAM65B bands as well as increases in their intensity (Fig. 3C,D). Moreover, in neutrophils lacking PLC β 2 or PLC β 3 and PI3K γ , in which both AKT and PKC activation by N-formylmethionyl-leucyl-phenylalanine (fMLP) are abrogated (Tang et al., 2011), the fMLP-induced upshift of the FAM65B bands and increases in the FAM65B intensity were significantly reduced (Fig. 3B). Furthermore, FAM65B could be phosphorylated *in vitro* by PKC α or AKT1 (supplementary material Fig. S2C). These results together suggest that FAM65B might be at least in part phosphorylated by PKC and AKT in fMLP-stimulated neutrophils. They also suggest that chemoattractant stimulation stabilizes the FAM65B protein. The observation that treatment of neutrophils with a proteasome inhibitor MG132 stabilizes FAM65B (Fig. 3D) suggests that chemoattractant-mediated phosphorylation of FAM65B might impede its degradation by the proteasomes.

When FAM65B was coexpressed with 14-3-3 β in HEK293 cells, increased expression of 14-3-3 β led to increased protein levels of FAM65B (Fig. 4A), suggesting that 14-3-3 proteins have a role in FAM65B stabilization. To determine whether the interaction between 14-3-3 and FAM65B depends on the

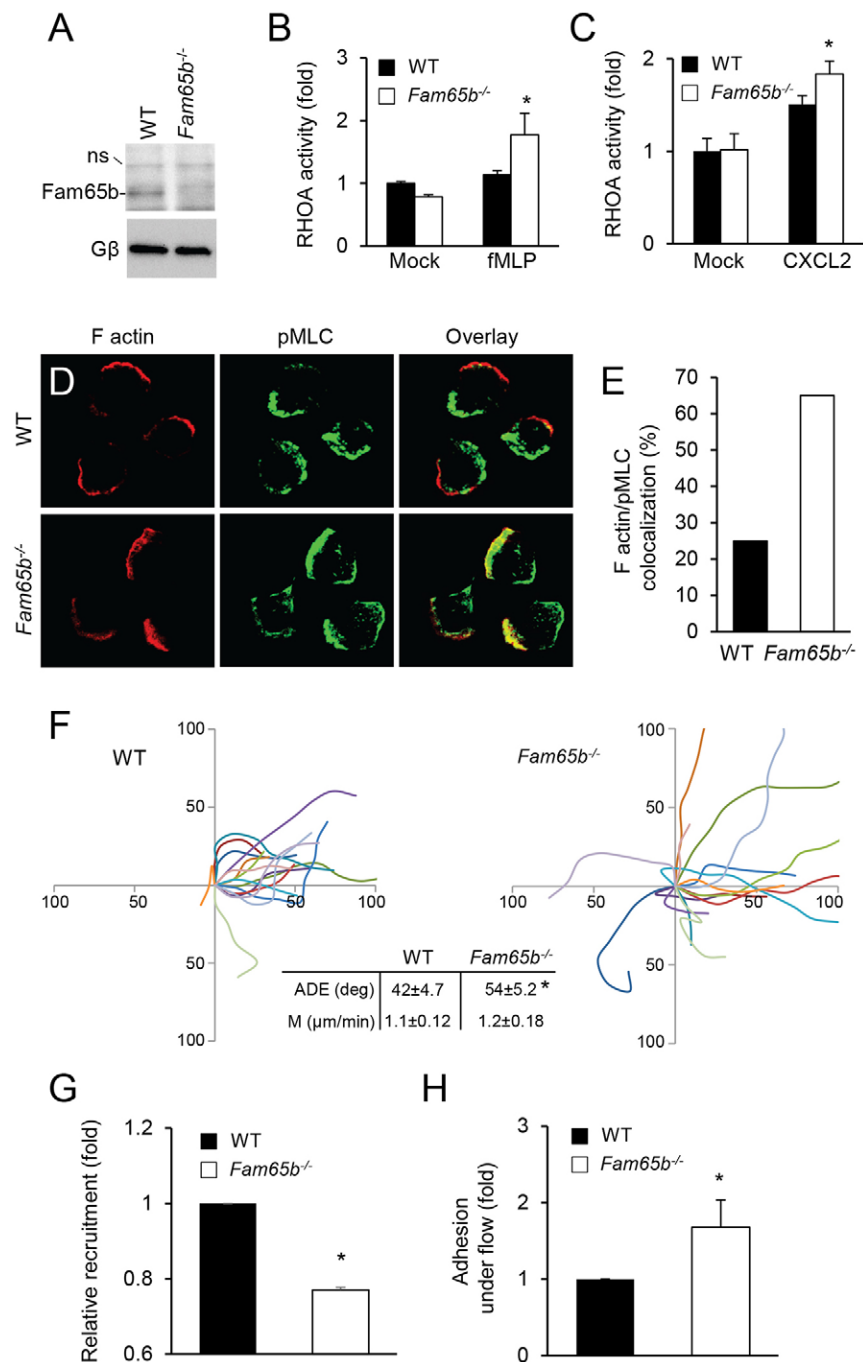


Fig. 2. FAM65B is a RHOA inhibitor in mouse neutrophils and regulates neutrophil polarization, chemotaxis and adhesion. (A) Western blotting analysis shows that mouse *Fam65b*^{-/-} neutrophils lacks FAM65B protein. ns, non-specific band. Gβ, the β2 subunit of heterotrimeric G protein. (B,C) FAM65B-deficiency results in elevated RHOA activity in response to chemoattractants. Neutrophils were stimulated with fMLP (200 nM) or CXCL2 (100 nM) for 3 min, followed by a G-LISA assay. Results are mean±s.d. (*n*=3). **P*<0.05 compared with the corresponding WT samples (Student's *t*-test). (D,E) FAM65B deficiency causes mislocalization of pMLC. Neutrophils were stimulated with fMLP (1 μM) for 3 min and stained with Alexa-Fluor-633–phalloidin and anti-pMLC antibody, followed with FITC-labeled secondary antibody. 50 WT and mutant cells were examined, and their polarization is plotted in E. (F) FAM65B-deficient neutrophils do not follow the gradient as well as the WT cells. Chemotaxis of WT and mutant neutrophils was assessed in a Dunn chamber coated with fibrinogen (100 μg/ml) in response to fMLP. Representative migration traces are shown. Chemotactic perimeters are shown in the inset. ADE, average directional error (smaller value means cells more accurately following the gradient); M, motility. The chemoattractant gradients are from right to left. Results are mean±s.e.m. (*n*>50). **P*<0.05 versus WT (paired Student's *t*-test). (G) FAM65B deficiency reduces neutrophil infiltration in a peritonitis model. Results are mean±s.d. (*n*=3). **P*<0.05 versus WT (Student's *t*-test). (H). FAM65B deficiency increases neutrophil adhesion to endothelial cells under flow. Results are mean±s.d. (*n*=3). **P*<0.05 versus WT (Student's *t*-test).

phosphorylation of these five putative phosphorylation sites and 14-3-3-binding motifs on FAM65B (supplementary material Fig. S2B), we generated a FAM65B mutant with these five Ser

residues being mutated to Ala, designated as FAM65B^{5A}. FAM65B^{5A}, which could hardly be phosphorylated *in vitro* by either PKCα or AKT1 (supplementary material Fig. S2C),

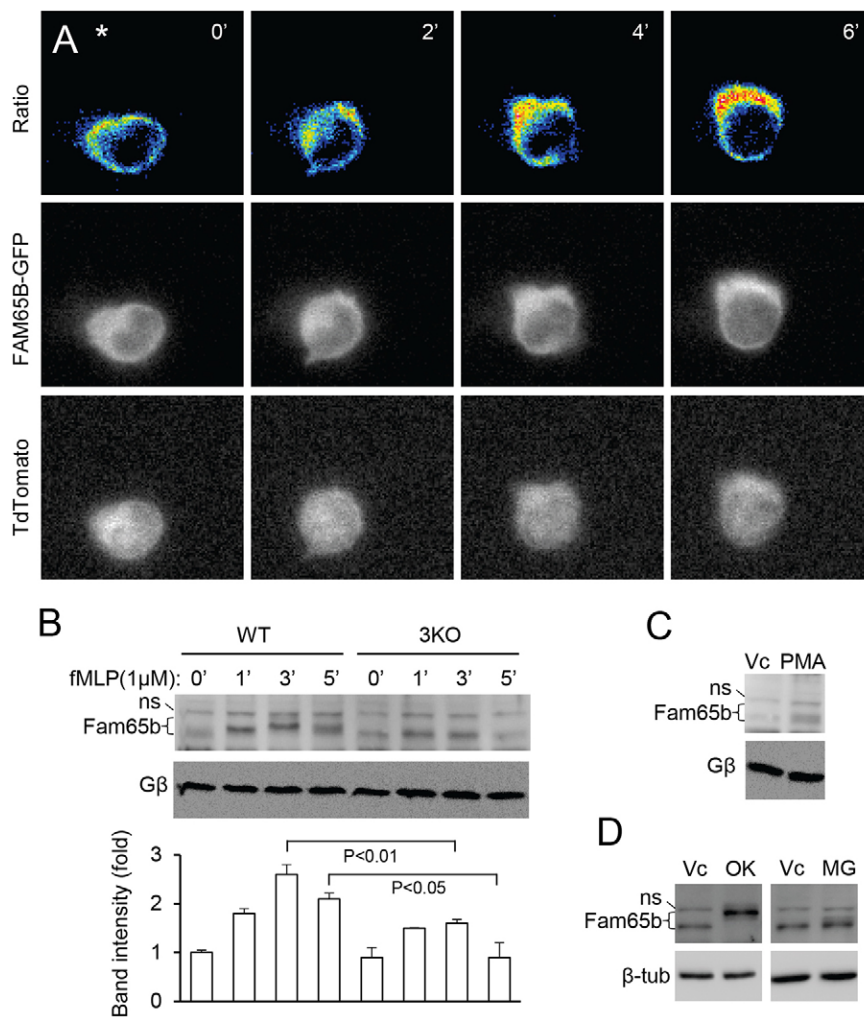


Fig. 3. Regulation of FAM65B by fMLP in neutrophils. (A) FAM65B–GFP is localized at the leading edge of a chemotaxing neutrophils. An fMLP gradient is applied from a micropipette in the direction marked by the asterisk. (B) FMLP regulates FAM65B electrophoretic mobility and stability in WT neutrophils, but significantly less in neutrophils lacking PLC β 2, PLC β 3 and PI3K γ (3KO). Relative FAM65B band intensities from three independent experiments are shown (Student *t*-test). ns, non-specific band. (C,D) Effect of PMA, okadaic acid (OK) and MG132 (MG) on FAM65B electrophoretic mobility and stability in neutrophils. G β , the β 2 subunit of heterotrimeric G protein Vc, vector control.

showed markedly reduced interaction with 14-3-3 β in a co-immunoprecipitation assay (Fig. 4B). When FAM65B^{5A} was coexpressed with 14-3-3 β , its stability was not affected by the presence of 14-3-3 (Fig. 4C; supplementary material Fig. S2D). Furthermore, ratio imaging of FAM65B^{5A}–GFP with coexpressed tdTomato or LifeAct–RFP showed that FAM65B^{5A}, unlike WT FAM65B, was no longer accumulated at the front of the cell upon fMLP stimulation despite some variations in its localization (Fig. 4D; supplementary material Fig. S2E; supplementary material Movie 3). Taken together with the fact that 14-3-3 β does not compete for binding of FAM65B to RHOA (Fig. 4E) nor blocks FAM65B-mediated inhibition of RHOA activity (supplementary material Fig. S2F), we believe that 14-3-3-mediated stabilization of FAM65B underlies a mechanism for fMLP to suppress RHOA activation at the front of a chemotaxing neutrophil.

DISCUSSION

Upon chemoattractant stimulation, neutrophils polarize, which is important for their directional migration. One of the hallmarks of neutrophil polarization is the localization of active RHOA and pMLC at the back of the cell. Our present study elucidates a mechanism for chemoattractant-induced polarization of active RHOA and pMLC in neutrophils and demonstrates a direct link from the front signals, which include PKC and AKT, to the

polarization. In this mechanism, chemoattractants stimulate the phosphorylation of FAM65B at the front, leading to its binding to 14-3-3 and stabilization. Accumulation of FAM65B at the front results in effective inhibition of RHOA at the leading edge, thus facilitating the establishment of the RHOA activity gradient needed for directional migration (Fig. 4F).

While the significance of PDZRhoGEF in mouse neutrophil function is unknown, Lfc deficiency largely abolishes RHOA activation in mouse neutrophils (Francis et al., 2006). Lfc deficiency also causes defects in chemotaxis directionality and adhesion, which are consistent with the phenotypes of FAM65B deficiency. The fact that Lfc localizes at both front and back of polarized mouse neutrophils provides the basis for RHOA activation in the front of neutrophils and a rationale for the existence of FAM65B there. Before neutrophils undergo chemotaxis, they have to extravasate out of the blood vessels. Neutrophil adhesion to the endothelium, in which RHOA has an important role (Xu et al., 2010), is required for the extravasation. Given adhesion is apolar, Lfc, which shows no polarized localization in neutrophils, is rather suited for this kind of apolar RHOA activation needed for adhesion. Shortly after adhesion, the cells would start to migrate either along or through the endothelium, and eventually in tissues. The migration requires polarization and a reduction in the strong adhesion needed to capture neutrophils that flow in the blood stream at high speeds.

Therefore, the inhibition of RHOA by FAM65B at the leading edge provides a mechanism to achieve the both purposes. On the one hand, the mechanism underlies the rapid polarization of RHOA activity that is uniformly activated by Lfc. This FAM65-mediated mechanism might be part of or interact with the aforementioned mechanisms mediated by mTORC2–PKC (Liu et al., 2010), PI3K (Van Keymeulen et al., 2006; Yoo et al., 2010), PDZRhoGEF (Wong et al., 2007) and possibly others, in sharpening and stabilizing the polarity. On the other hand, the mechanism reduces the adhesion (Fig. 2H), which would otherwise compromise *in vivo* neutrophil recruitment (Fig. 2G).

Our evidence demonstrates that the front signaling pathways, including the PLC β –PKC and PI3K γ –Akt pathways, are involved in the phosphorylation of FAM65B, leading to its stabilization. Other protein kinases might also participate, as neither upshift nor accumulation of FAM65B protein induced by fMLP was completely abrogated in neutrophils lacking PLC β 2, PLC β 3 and PI3K γ (Fig. 3B). In an *in vitro* kinase assay, RSK, in addition to PKC and AKT, could also phosphorylate FAM65B (supplementary material Fig. S2C). Some of the phosphorylation sites on FAM65B also match the substrate motifs of other protein kinases that can be potentially activated by chemoattractants. These include PAK, MAPAKPK, SGK and PKA, to name a few. Many of these kinases can be directly or indirectly activated by the front signaling pathways that also include RAC and CDC42 proteins. Although phosphorylation and stabilization of FAM65B might not be the sole mechanism for its accumulation at the leading edge, this study provides a sound example of ‘local inhibition and global excitation’ for back polarization that extends the ‘local excitation and global inhibition’ (‘LEGI’) theory proposed by Devreotes and Iglesias (Ma et al., 2004) for the understanding of chemotactic cell polarization.

This study confirms that FAM65B protein is a RHOA regulator *in vitro*. We also identified a RHOA-binding motif (RBM), which is conserved in the FAM65 family of proteins. A region upstream of the RBM was identified by Rougerie et al. (Rougerie et al., 2013) for RHOA binding. Although an involvement of this region in neutrophil function cannot be completely excluded, it is not the primary RHOA-binding site for FAM65B. In addition, this study shows that FAM65B is a physiologically significant RHOA inhibitor in neutrophils (Fig. 2B,C). The insignificant effect of FAM65B deficiency on RHOA activation at high concentrations of chemoattractants (supplementary material Fig. S1D) might be due to rapid FAM65B polarization under these conditions. Once FAM65B is polarized to the front, it would not inhibit RHOA in most parts of the cell, where it is absent. Furthermore, this present study reveals a mechanism for acute regulation of the FAM65B protein level in response to stimulation through phosphorylation-dependent 14-3-3 protein binding in addition to transcription-based regulation (Rougerie et al., 2013). Given that the RBM is shared by the other two members of this family, it is likely that FAM65A and FAM65C are also RHOA inhibitors. It is also possible that FAM65 proteins regulate other close RHOA homologs. This notion is supported by the observation that expression of FAM65B^{5A} causes neutrophil body elongation accompanied by the trends in improvement in directionality and motility (supplementary material Fig. S3), phenotypes also exhibited upon genetic inactivation of all of the RHO isoforms (Königs et al., 2014). Thus, the FAM65 family of proteins might constitute a new class of RHO regulators. As members of this family are broadly expressed in many tissues and cell types, we

anticipate that this family of proteins will have broad physiological and pathophysiological functions. Indeed, a mutation in the human FAM65B gene has recently been associated with hearing loss (Diaz-Horta et al., 2014). Future studies are needed to determine whether the phenotype is related to RHOA regulation.

MATERIALS AND METHODS

Mice and reagents

Fam65b^{-/-} mice were generated at the Mutant Mouse Regional Resource Center (UC Davis) from the knockout mouse project using ESC clone 15686A-B6, in which exons 2–14 of the *Fam65b* gene are deleted. The mice are maintained in the C57BL/6 background. The mouse line lacking PLC β 2, PLC β 3 and PI3K γ has previously been described (Tang et al., 2011). All of the animal studies were approved by the institutional animal care and use committees of Yale University.

Antibodies were obtained from various commercial sources: FAM65B (17015-1-AP; Proteintech), RHOA (sc-418; Santa Cruz Biotechnology), CDC42 (sc-87; Santa Cruz Biotechnology), RAC1 (Santa Cruz Biotechnology), 14-3-3 α and 14-3-3 β (1062-1; Epitomics), 14-3-3 ϵ (2784-1; Epitomics), 14-3-3 θ (Epitomics; 3887-1), pMLC (Cell Signaling). Alexa-Fluor-488-labeled phalloidin was obtained from Invitrogen.

The FAM65B cDNA was purchased from Genecopoeia Inc., and subcloned into pCIN4-FLAG–HA, pCMV–Myc and pEGFP vectors. The FAM65B mutant (5SA) was generated using site-specific mutagenesis kit (Stratagene, USA).

Protein purification for mass spectrometry analysis

An HEK293 cell line was established for stable expression of FAM65B using the vector pCIN4-FLAG–HA–FAM65B. Cells were lysed in the buffer containing 0.5% NP40 10 mM HEPES pH 7.9, 10 mM KCl, 0.1 mM EDTA, 1 mM DTT, 0.5 mM PMSF, and protein inhibitor mixture, and incubated with anti-FLAG (M2 clone) antibody-conjugated agarose. The bound polypeptides were eluted with the FLAG peptide and subjected to further affinity purification using the anti-HA-antibody-conjugated agarose. The final eluate was immunoprecipitated with the HA peptide and resolved by SDS-PAGE on a 4–20% gradient gel, followed by Colloidal Blue staining. Bands were excised for analysis by mass spectrometry.

Neutrophil preparation, transfection and staining

Mouse neutrophils were purified from bone marrow as previously described (Tang et al., 2011; Xu et al., 2010; Zhang et al., 2013). Briefly, bone marrow cells collected from mice were treated with ACK buffer (155 mM NH₄Cl, 10 mM KHCO₃ and 127 μ M EDTA) for red blood cell lysis, followed by a discontinuous Percoll density gradient centrifugation. Neutrophils were collected from the band located between 81% and 62% of Percoll.

For transient transfection of primary mouse neutrophils, 3 \times 10⁶ neutrophils were electroporated with 1.6 μ g endotoxin-free plasmid using the human monocyte nucleofection kit with the Amaxa system. The cells were then cultured for 4 h in the medium supplied with the kit containing 10% FBS and 25 ng/ml recombinant GM-CSF. Before the cells were used for experiments, they were incubated in HBSS containing 0.2% BSA on ice for 1 h.

For staining, neutrophils were placed onto the coverslips for 15 min before stimulation. The cells were then fixed with 4% paraformaldehyde and permeabilized with 0.2% Triton X-100 in PBS. Mounted slides were observed under a confocal microscopy (Leica SP5). Staining of neutrophils with various antibodies was carried out as previously described (Xu et al., 2010).

In vitro chemotaxis assay with a micropipette or a Dunn chamber

For application of a chemoattractant gradient using a micropipette, an Eppendorf Femotip was loaded with 100 μ M fMLP, and an fMLP gradient was maintained by applying a pressure to the micropipette using

an Eppendorf FemtoJet microinjection system. The tip of the micropipette was placed and attempted to stay at 50 μm from targeted cells. Time-lapse image series were acquired using an automatic Olympus IX71 inverted microscope with a 60 \times oil objective at 30-s intervals.

The chemotaxis assay using a Dunn chamber was carried out as previously described (Zicha et al., 1997) with some modifications as detailed previously (Xu et al., 2010; Zhang et al., 2010). We analyzed wild-type and mutant neutrophils simultaneously by labeling the cells with different tracing dyes. We alternated the labeled group in the study to completely eliminate the possibility of any influence from the dye. In addition, free fluorescein isothiocyanate was mixed with chemoattractants to monitor the gradient. Only cells under similar gradients were analyzed, and chemotaxis perimeters were calculated as previously published (Zhang et al., 2010). Time-lapse image series were acquired at 30-s intervals for 30 min.

In vivo neutrophil infiltration into inflamed peritonea

Purified wild-type and mutant neutrophils were labeled with 0.75 μM CFSE and 0.37 μM Far-Red DDAO SE, respectively, and vice versa. These cells were mixed at a 1:1 ratio and administered into wild-type littermates via retro-orbital injection, which received peritoneal injection of 1 ml 3% Thioglycolate one and half hour earlier. The mice were euthanized two and half h later. Cells in their peritonea were collected and analyzed by cell counting and flow cytometry.

Flow chamber assay

Mouse endothelial cells (Wang et al., 2008) were cultured to confluency on fibronectin-coated coverslips and treated with 50 ng/ml TNF α for 4 h. The coverslips containing the endothelial cell layer were washed with PBS and placed in a flow chamber apparatus (GlycoTech). Purified wildtype and mutant neutrophils were first labeled with CFSE and Calcein Red-Orange AM Dyes (Invitrogen), respectively, at 37 $^{\circ}\text{C}$ for 15 mins and then mixed at a 1:1 ratio. The mixed neutrophils were placed on top of the endothelial cells and subjected to sheer flow of 1 dyne/cm 2 for 10 min. The cells were then fixed, and the number of neutrophils adhering to the endothelial cells was counted using a fluorescence microscope.

Immunoprecipitation

HEK293 cells were maintained in Dulbecco's modified Eagle's medium (DMEM) with 4.5 g/l glucose supplemented with 10% fetal bovine serum (FBS). Transient transfection was carried out using Lipofectamine Plus (Life Technologies, Grand Island, NY), and samples were collected 24 h after transfection. Cells were lysed in a cell lysis buffer [20 mM Tris-HCl pH 7.5, 150 mM NaCl, 1% NP-40, 5 mM EDTA, Roche's protease inhibitor cocktail, Roche's phosphatase inhibitor cocktail (Indianapolis, IN)]. After removing insoluble materials by centrifugation, immunoprecipitation was carried out by adding various antibodies and Protein A/G-PLUS-agarose beads into supernatants. Immunocomplexes were washed three times with lysis buffer before the SDS sample buffer was added for SDS-PAGE analysis.

Guanine-nucleotide-loading assays

The effect of FAM65B on loading of N-methylanthraniloyl-GTP (Mant-GTP, from JENA Bioscience) to recombinant RHOA was performed as previously described (Rojas et al., 2003; Wang et al., 2009). In brief, purified RHOA (0.2 μM) was incubated in an assay buffer containing 20 mM Tris-HCl pH 7.5, 150 mM NaCl, 5 mM MgCl $_2$ and 1 mM dithiothreitol with 0.5 μM Mant-GTP in the presence or absence of 0.2 μM recombinant FAM65B. Immediately after mixing, the fluorescence intensity was determined by using a fluorometer (Wallac Vector, 1420 multilabel counter) with the excitation wavelength of 360 nm and emission wavelength of 440 nm.

Luciferase reporter assays

HEK293 cells were seeded in 24-well culture plates and transfected with the luciferase reporter construct SRE-luc, the GFP normalization plasmid

and other plasmids, as shown in the figures, by using Lipofectamine Plus. After transfection, cells were cultured in serum-free medium for 24 h before the GFP intensity was measured by using a fluorometer. The cells were then lysed, and their luciferase activities were determined by using a luminometer. Data are presented after the luciferase activity was normalized against the GFP intensity.

Determination of active RHOA level

The levels of active GTP-bound RHOA were determined using a G-LISA RHOA activation assay kit (Cytoskeleton, Inc.) or RBD-pulldown assays. For G-LISA, 10 6 neutrophils were stimulated with mock or ligands for 3 min before the assay. For the GST pulldown assay, 3 \times 10 6 cells were lysed with the lysis buffer (50 mM Tris-HCl pH 7.3, 10 mM MgCl $_2$ and 0.2M NaCl, 2% NP40, 10% glycerol, 2 mM orthovanadate) containing recombinant GST-Rhotekin-RBD. Bound GTPases were detected by western blotting analysis.

GST-FAM65B protein preparation and kinase assay

GST-FAM65B (WT or 5SA) in the pGEX-4T-2 vector was purified from *E. coli* using glutathione-agarose (Sigma). The recombinant protein kinases AKT1, RSK1 and PKC α were purchased from Carna Biosciences (Kobe, Japan). GST-FAM65B (WT or 5SA) and recombinant kinases were incubated in a kinase buffer containing 50 mM Tris-HCl pH 7.5, 10 mM manganese chloride and 100 mM [γ - ^{32}P]ATP (500 c.p.m./ μmol). After incubation for 30 min at 30 $^{\circ}\text{C}$, the reactions were terminated by addition of SDS sample buffer, and the reaction samples were separated by SDS-PAGE and analyzed by Ponceau S staining and autoradiography.

Acknowledgements

We thank Michelle Orsulak for technical assistance.

Competing interests

The authors declare no competing or financial interests.

Author contributions

K.G., W.T., Y.L., P.Z., D.W., and C.W. performed the experiments. K.G., L.Y., C.W., and D.Q.W. designed the experiments and analyzed the results. C.W. and D.Q.W. wrote the manuscript.

Funding

This work is supported by the National Institutes of Health (NIH) [grant numbers HL108430, HL120465 to D.W.]; an AHA Early Investigator Award (to W.T.); the National Natural Science Foundation of China [grant numbers 31400753 to K.G., 31071193 to L.Y., 81171964 to C.J.]; and a China Postdoctoral Science Foundation Grant [grant number 2013M541461 to K.G.]. Deposited in PMC for release after 12 months.

Supplementary material

Supplementary material available online at <http://jcs.biologists.org/lookup/suppl/doi:10.1242/jcs.161497/-DC1>

References

- Bourne, H. R. and Weiner, O. (2002). A chemical compass. *Nature* **419**, 21.
- Dakour, J., Li, H. and Morrish, D. W. (1997). PL48: a novel gene associated with cytotrophoblast and lineage-specific HL-60 cell differentiation. *Gene* **185**, 153–157.
- Diaz-Horta, O., Subasioglu-Uzak, A., Grati, M., DeSmidt, A., Foster, J., II, Cao, L., Bademci, G., Tokgoz-Yilmaz, S., Duman, D., Cengiz, F. B. et al. (2014). FAM65B is a membrane-associated protein of hair cell stereocilia required for hearing. *Proc. Natl. Acad. Sci. USA* **111**, 9864–9868.
- Francis, S. A., Shen, X., Young, J. B., Kaul, P. and Lerner, D. J. (2006). Rho GEF Lsc is required for normal polarization, migration, and adhesion of formyl-peptide-stimulated neutrophils. *Blood* **107**, 1627–1635.
- Giagulli, C., Scarpini, E., Ottoboni, L., Narumiya, S., Butcher, E. C., Constantin, G. and Laudanna, C. (2004). RhoA and zeta PKC control distinct modalities of LFA-1 activation by chemokines: critical role of LFA-1 affinity triggering in lymphocyte in vivo homing. *Immunity* **20**, 25–35.
- Graziano, B. R. and Weiner, O. D. (2014). Self-organization of protrusions and polarity during eukaryotic chemotaxis. *Curr. Opin. Cell Biol.* **30**, 60–67.
- Hill, C. S., Wynne, J. and Treisman, R. (1995). The Rho family GTPases RhoA, Rac1, and CDC42Hs regulate transcriptional activation by SRF. *Cell* **81**, 1159–1170.
- Hirayama, E. and Kim, J. (2008). Identification and characterization of a novel neural cell adhesion molecule (NCAM)-associated protein from quail myoblasts:

- relationship to myotube formation and induction of neurite-like protrusions. *Differentiation* **76**, 253–266.
- Honing, H., van den Berg, T. K., van der Pol, S. M., Dijkstra, C. D., van der Kammen, R. A., Collard, J. G. and de Vries, H. E. (2004). RhoA activation promotes transendothelial migration of monocytes via ROCK. *J. Leukoc. Biol.* **75**, 523–528.
- Iden, S. and Collard, J. G. (2008). Crosstalk between small GTPases and polarity proteins in cell polarization. *Nat. Rev. Mol. Cell Biol.* **9**, 846–859.
- Königs, V., Jennings, R., Vogl, T., Horsthemke, M., Bachg, A. C., Xu, Y., Grobe, K., Brakebusch, C., Schwab, A., Bähler, M. et al. (2014). Mouse macrophages completely lacking Rho subfamily GTPases (RhoA, RhoB, and RhoC) have severe lamellipodial retraction defects, but robust chemotactic navigation and altered motility. *J. Biol. Chem.* **289**, 30772–30784.
- Li, Z., Hannigan, M., Mo, Z., Liu, B., Lu, W., Wu, Y., Smrcka, A. V., Wu, G., Li, L., Liu, M. et al. (2003). Directional sensing requires G beta gamma-mediated PAK1 and PIX alpha-dependent activation of Cdc42. *Cell* **114**, 215–227.
- Li, Z., Dong, X., Wang, Z., Liu, W., Deng, N., Ding, Y., Tang, L., Hla, T., Zeng, R., Li, L. et al. (2005). Regulation of PTEN by Rho small GTPases. *Nat. Cell Biol.* **7**, 399–404.
- Liu, L. and Parent, C. A. (2011). Review series: TOR kinase complexes and cell migration. *J. Cell Biol.* **194**, 815–824.
- Liu, L., Das, S., Losert, W. and Parent, C. A. (2010). mTORC2 regulates neutrophil chemotaxis in a cAMP- and RhoA-dependent fashion. *Dev. Cell* **19**, 845–857.
- Ma, L., Janetopoulos, C., Yang, L., Devreotes, P. N. and Iglesias, P. A. (2004). Two complementary, local excitation, global inhibition mechanisms acting in parallel can explain the chemoattractant-induced regulation of PI(3,4,5)P3 response in dictyostelium cells. *Biophys. J.* **87**, 3764–3774.
- Onsum, M. D. and Rao, C. V. (2009). Calling heads from tails: the role of mathematical modeling in understanding cell polarization. *Curr. Opin. Cell Biol.* **21**, 74–81.
- Riedl, J., Crevenna, A. H., Kessenbrock, K., Yu, J. H., Neukirchen, D., Bista, M., Bradke, F., Jenne, D., Holak, T. A., Werb, Z. et al. (2008). Lifeact: a versatile marker to visualize F-actin. *Nat. Methods* **5**, 605–607.
- Rojas, R. J., Kimple, R. J., Rossman, K. L., Siderovski, D. P. and Sondek, J. (2003). Established and emerging fluorescence-based assays for G-protein function: Ras-superfamily GTPases. *Comb. Chem. High Throughput Screen* **6**, 409–418.
- Rougerie, P., Largeteau, Q., Megrelis, L., Carrette, F., Lejeune, T., Toffali, L., Rossi, B., Zeghouf, M., Cherfils, J., Constantin, G. et al. (2013). Fam65b is a new transcriptional target of FOXO1 that regulates RhoA signaling for T lymphocyte migration. *J. Immunol.* **190**, 748–755.
- Srinivasan, S., Wang, F., Glavas, S., Ott, A., Hofmann, F., Aktories, K., Kalman, D. and Bourne, H. R. (2003). Rac and Cdc42 play distinct roles in regulating PI(3,4,5)P3 and polarity during neutrophil chemotaxis. *J. Cell Biol.* **160**, 375–385.
- Tang, W., Zhang, Y., Xu, W., Harden, T. K., Sondek, J., Sun, L., Li, L. and Wu, D. (2011). A PLCβ/PI3Kγ-GSK3 signaling pathway regulates cofilin phosphatase slingshot2 and neutrophil polarization and chemotaxis. *Dev. Cell* **21**, 1038–1050.
- Van Keymeulen, A., Wong, K., Knight, Z. A., Govaerts, C., Hahn, K. M., Shokat, K. M. and Bourne, H. R. (2006). To stabilize neutrophil polarity, PIP3 and Cdc42 augment RhoA activity at the back as well as signals at the front. *J. Cell Biol.* **174**, 437–445.
- Wang, F. (2009). The signaling mechanisms underlying cell polarity and chemotaxis. *Cold Spring Harb. Perspect. Biol.* **1**, a002980.
- Wang, Z., Liu, B., Wang, P., Dong, X., Fernandez-Hernando, C., Li, Z., Hla, T., Li, Z., Claffey, K., Smith, J. D. et al. (2008). Phospholipase C beta3 deficiency leads to macrophage hypersensitivity to apoptotic induction and reduction of atherosclerosis in mice. *J. Clin. Invest.* **118**, 195–204.
- Wang, Z., Kumamoto, Y., Wang, P., Gan, X., Lehmann, D., Smrcka, A. V., Cohn, L., Iwasaki, A., Li, L. and Wu, D. (2009). Regulation of immature dendritic cell migration by RhoA guanine nucleotide exchange factor Arhgef5. *J. Biol. Chem.* **284**, 28599–28606.
- Wong, K., Van Keymeulen, A. and Bourne, H. R. (2007). PDZRhoGEF and myosin II localize RhoA activity to the back of polarizing neutrophil-like cells. *J. Cell Biol.* **179**, 1141–1148.
- Wu, D. (2005). Signaling mechanisms for regulation of chemotaxis. *Cell Res.* **15**, 52–56.
- Xu, J., Wang, F., Van Keymeulen, A., Herzmark, P., Straight, A., Kelly, K., Takuwa, Y., Sugimoto, N., Mitchison, T. and Bourne, H. R. (2003). Divergent signals and cytoskeletal assemblies regulate self-organizing polarity in neutrophils. *Cell* **114**, 201–214.
- Xu, W., Wang, P., Petri, B., Zhang, Y., Tang, W., Sun, L., Kress, H., Mann, T., Shi, Y., Kubes, P. et al. (2010). Integrin-induced PIP5K1C kinase polarization regulates neutrophil polarization, directionality, and in vivo infiltration. *Immunity* **33**, 340–350.
- Yoo, S. K., Deng, Q., Cavnar, P. J., Wu, Y. I., Hahn, K. M. and Huttenlocher, A. (2010). Differential regulation of protrusion and polarity by PI3K during neutrophil motility in live zebrafish. *Dev. Cell* **18**, 226–236.
- Yoon, S., Molloy, M. J., Wu, M. P., Cowan, D. B. and Gussoni, E. (2007). C6ORF32 is upregulated during muscle cell differentiation and induces the formation of cellular filopodia. *Dev. Biol.* **301**, 70–81.
- Zhang, Y., Tang, W., Jones, M. C., Xu, W., Halene, S. and Wu, D. (2010). Different roles of G protein subunits beta1 and beta2 in neutrophil function revealed by gene expression silencing in primary mouse neutrophils. *J. Biol. Chem.* **285**, 24805–24814.
- Zhang, Y., Tang, W., Zhang, H., Niu, X., Xu, Y., Zhang, J., Gao, K., Pan, W., Boggon, T. J., Toomre, D. et al. (2013). A network of interactions enables CCM3 and STK24 to coordinate UNC13D-driven vesicle exocytosis in neutrophils. *Dev. Cell* **27**, 215–226.
- Zicha, D., Dunn, G. and Jones, G. (1997). Analyzing chemotaxis using the Dunn direct-viewing chamber. *Methods Mol. Biol.* **75**, 449–457.

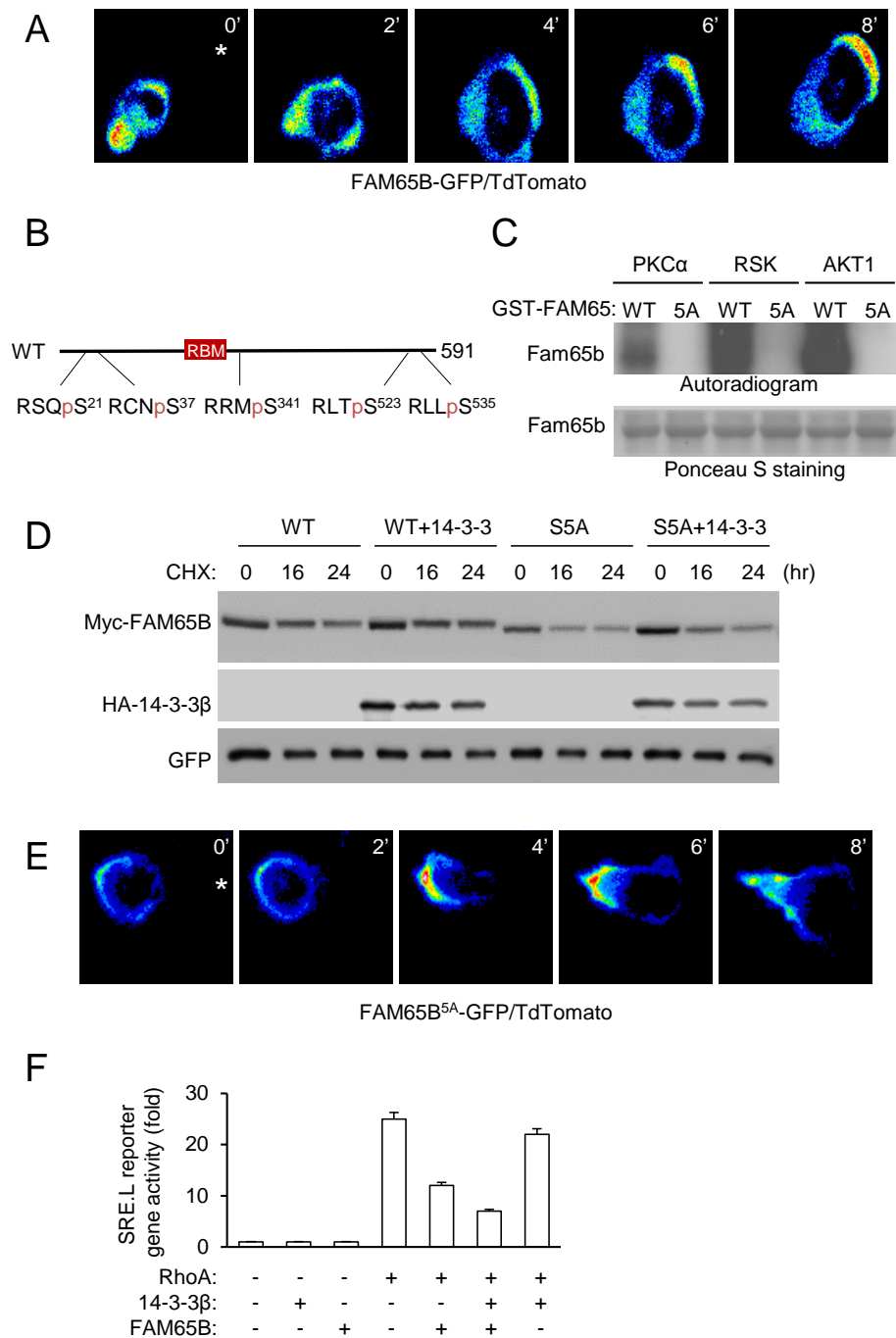


Figure S2. Supplementary data for Figure 3 and 4. **A,E.** Additional cells showing the localization of FAM65B-GFP (**A**) and FAM65B^{5A}-GFP (**E**). **B.** Phosphorylation sites on FAM65B identified by MS. **C.** In vitro phosphorylation of FAM65B. Recombinant GST-FAM65B proteins were subjected to phosphorylation by recombinant PKCα, RSK and AKT1 in an in vitro kinase assay using [³²P]γATP. **D.** Representative Western blotting images for Fig. 4C. **F.** The 14-3-3 protein does not decrease the inhibitory effect of FAM65B on RHOA-induced activation of the SRE.L reporter gene in HEK293 cells.

	RFP	Fam65b ^{5A}
ADE (deg)	49±5.2	41±4.3
M (µm/min)	1.1±0.21	1.4±0.19

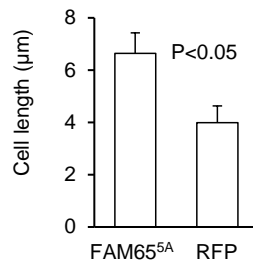


Figure S3. Effect of expression of FAM65B^{5A} mutant on neutrophil chemotaxis. Mouse neutrophils were transfected with RFP and FAM65B^{5A}-GFP, respectively, and mixed at 1:1 ratio followed by the chemotaxis assay in a Dunn chamber as described in Fig. 2F. Chemotactic parameters including ADE (average directional error) and motility (motility) as well as cell body length are shown (Student's t-test, n>30).



Movie 1: A representative movie shows neutrophil migration in a Dunn chamber under an fMLP gradient. Equal numbers of WT (labelled with a red dye) and FAM65B-null (labelled with a green dye) neutrophils were mixed and subjected to the chemotaxis assay. The first image is the overlay of fluorescent and phase-contrast images to allow genotype identification. The rest of time-lapses images were taken under the phase contrast setting. The fMLP gradient is from right to left.



Movie 2



Movie 3

Movie 2 and 3: Localization of FAM65B-GFP and LifeAct-RFP in mouse neutrophils. Neutrophils expressing WT FAM65B-GFP (Movie 2) or FAM65B^{5A}-GFP (Movie 3) were stimulated by fMLP from a micropipette whose location is marked by the red dot in the first image.